Microchimica Acta (2020) 187:197
https://doi.org/10.1007/s00604-020-4169-z

ORIGINAL PAPER

A colorimetric immunosensor for determination of foodborne bacteria using rotating immunomagnetic separation, gold nanorod indication, and click chemistry amplification

Ruya Guo[1] · Fengchun Huang[1] · Gaozhe Cai[1] · Lingyan Zheng[2] · Li Xue[2] · Yanbin Li[3] · Ming Liao[4] · Maohua Wang[2] · Jianhan Lin[2]

Received: 16 September 2019 / Accepted: 13 February 2020

Abstract

A colorimetric immunosensor was developed for the determination of *Salmonella* Typhimurium using rotating magnetic separation, gold nanorod (GNR) indication, and click chemistry amplification. The target bacteria were first separated from large-volume sample using a rotating magnetic field and a small amount (50 μg) of immunomagnetic nanoparticles (MNPs), resulting in the forming of magnetic bacteria. Then, the magnetic bacteria were conjugated with catalase (CAT)-labeled antibodies, which were synthesized using trans-cyclooctene/1,2,4,5-tetrazine click chemistry reaction, resulting in the forming of enzymatic bacteria. Then the CATs on the enzymatic bacteria were used to decompose an excessive amount of hydrogen peroxide (H_2O_2), the remaining H_2O_2 was mixed with horseradish peroxidase to etch the GNRs, resulting in color change and absorbance peak shift of the GNRs. Finally, the peak shift was measured and analyzed for the quantitative determination of target bacteria. This immunosensor was able to detect *Salmonella* Typhimurium with a linear range of 10^1–10^5 CFU mL^{-1} in 3 h with a low detection limit of 35 CFU mL^{-1}. The mean recovery for *Salmonella* Typhimurium in spiked chicken samples was 109%.

Keywords Immunosensor · Biosensor · Rotating magnetic field · Immunomagnetic separation · Gold nanorod · Gold nanoparticle etching · Spiral channel · *Salmonella* detection · Food safety

Introduction

Foodborne diseases caused by pathogens have seriously threatened public health and resulted in enormous economic losses [1]. As a kind of well-known foodborne pathogen, *Salmonella* often causes food and environmental contaminations. It can trigger some zoonotic diseases, such as gastroenteritis, typhoid, and even death [2, 3]. So far, plate colony counting (culture) [4], enzyme-linked immunosorbent assay (ELISA) [5], and polymerase chain reaction (PCR) [6] are considered as the gold standard or recommended methods for *Salmonella* detection. However, these methods suffer from some inherent limitations, such as long detection time, insufficient sensitivity, or complex DNA extraction procedures. Thus, it is of great significance to develop fast, sensitive, and in-field methods for *Salmonella* detection to ensure food safety.

To achieve visual detection of biological targets, recently reported strategies and applications using colorimetric sensors based on etching and growth of noble metal nanoparticles have been well summarized [7]. Gold nanoparticles are excellent noble metal signal probes and have been often used for *salmonella* detection [8, 9]. They also possess higher extinction coefficients and more vivid colors compared to traditional organic dyes [10]. Among them, gold nanorods (GNRs) have

Electronic supplementary material The online version of this article (https://doi.org/10.1007/s00604-020-4169-z) contains supplementary material, which is available to authorized users.

✉ Jianhan Lin
jianhan@cau.edu.cn

[1] Key Laboratory of Agricultural Information Acquisition Technology, Ministry of Agriculture and Rural Affairs, China Agricultural University, Beijing 100083, China

[2] Key Laboratory of Modern Precision Agriculture System Integration Research, Ministry of Education, China Agricultural University, Beijing 100083, China

[3] Department of Biological and Agricultural Engineering, University of Arkansas, Fayetteville, AR 72701, USA

[4] College of Veterinary Medicine, South China Agricultural University, Guangzhou 510642, China

Published online: 03 March 2020

exhibited robust color change after being etched by some oxidants [11]. For instance, a multicolor aptasensor was developed for visual detection of ochratoxin A using TMB^{2+} as an oxidant to etch GNRs [12]. Besides, hydroxyl radical (•OH), which is generally functionalized through the catalytic reaction of hydrogen peroxide (H_2O_2) using Fenton's reagent, has a strong oxidation ability to etch GNRs [13]. Additionally, horseradish peroxidase (HRP) was demonstrated to own a higher catalytic activity with H_2O_2 than Fenton's reagent at low concentration of H_2O_2 (< 0.1 M) and room temperature [14], and a highly sensitive colorimetric assay was proposed for detection of physiological glucose using HRP-induced GNR etching [15]. To further improve the sensitivity, some signal amplification strategies were reported based on click chemistry and enzyme catalysis with good biocompatibility, rapidness, and flexibility [16, 17]. As classical click chemistry molecules, trans-cyclooctene (TCO), and 1,2,4,5-tetrazine (Tz) have received much attention due to their high reaction rate and biocompatibility for effective signal amplification [18, 19]. These click molecules can be coupled with some proteins (enzymes, antibodies, etc.) based on the reaction between the N-hydroxysuccinimide-activated TCO/Tz (NHS-TCO/Tz) and the amine group ($–NH_2$) on the proteins [20, 21]. For example, Jiang et al. successfully synthesized HRP assemblies by the click chemistry reaction between TCO-HRP and Tz-HRP, which greatly amplified the signals to enhance the sensitivity [22]. Therefore, it might be promising to develop sensitive sensors combining HRP-induced GNR etching and click chemistry for visual detection of foodborne pathogens.

Immunomagnetic separation (IMS) is an effective technology for purification and pre-concentration of target pathogens from complex food samples and often combined with various biosensors to enhance the detection sensitivity and reduce the background noises [23]. Conventional IMS can generally handle only a small volume of samples in 1.5 mL centrifuge tube manually due to the limited working range of magnetic field [24]. Additionally, pathogenic bacteria always exist at low concentration and with heterogeneous distribution in real food samples for routine screening. Recently, some efforts on novel IMS methods for a large volume of food samples were made to improve the detection sensitivity and signal-to-noise ratio. Lee et al. proposed an immunomagnetic flow assay for the rapid separation of pathogenic bacteria from a large volume of food samples using a 3D-printed cylindrical channel [25]. This assay was demonstrated to be able to separate the target bacteria from 10 mL of sample in 1 min. However, a large amount (200 μg) of the immune magnetic nanoparticles (MNPs) for each test at high cost might greatly limit its practical application. Besides, some studies on continuous-flow IMS were reported based on the forming of MNP chains or clusters using soft magnetic materials with special structure, such as mu-metal foils [26], sawtooth-shaped iron foils [27], and iron shots [28]. However, the static and heterogeneous distribution of the MNPs in the channel might lead to low separation efficiency. Thus, it might be effective and practical to improve the separation efficiency using a small amount of moving MNP chains or clusters to capture the target bacteria.

In this study, we proposed a colorimetric immunosensor for the quantitative determination of *Salmonella* using moving immune MNPs for specific separation of bacteria from large volume, TCO-Tz click reaction for efficient amplification of biological signal, and GNRs for visible indication of detection result. As shown in Fig. 1, the capture antibodies (CAbs) modified MNPs were first injected into a spiral channel and captured at the presence of an anti-clockwise rotating high gradient magnetic field. Then, 10 mL of bacterial sample was clockwise injected into the channel and captured by the immune MNPs due to the antibody-antigen reaction to form the magnetic bacteria in 1 mL of PBS. Subsequently, the detection antibodies (DAbs) were modified with catalases (CATs) by the TCO/Tz click chemistry and incubated with the magnetic bacteria to form the enzymatic bacteria. After that, an excessive amount of H_2O_2 was added and in part decomposed by the CATs on the enzymatic bacteria. Finally, the remaining H_2O_2 was used with HRP to induce the etching of GNRs, resulting in the change on the color of GNRs from dark blue to pink, and the absorbance peak shift was measured to determine the concentration of *Salmonella*.

Materials and methods

Materials

Gold(III) chloride trihydrate ($HAuCl_4$) from Sigma Aldrich (St. Louis, MO, USA, https://www.sigmaaldrich.com), Sodium borohydride ($NaBH_4$), L-ascorbic acid (AA) from Aladdin (Shanghai, China, https://www.aladdin-e.com), Silver nitrate ($AgNO_3$) from Sinopharm Chemical (Shanghai, China, http://www.sinopharmholding.com), and cetyltrimethylammonium bromide (CTAB) from Amresco (Solon, OH, USA, http://www.amresco-inc.com) were used for the synthesis of GNRs. Hydrogen peroxide (H_2O_2), N-(3-dimethylaminopropyl)-N′-ethylcarbodiimide hydrochloride (EDC·HCl) and N-hydroxysulfosuccinimide sodium (NHSS) were purchased from Aladdin. Phosphate buffered saline (PBS, 0.01 M, pH 7.2–7.4) and horseradish peroxidase were purchased from Solarbio (Beijing, China, http://www.solarbio.com). Tween-20 from Amresco was prepared in PBS for washing. Bovine serum albumin (BSA, 1%, *w*/*v*) from EM Science (Gibbstown, NJ, USA, http://www.emscience.com) was prepared in PBS for blocking. Bovine liver catalase from Sigma Aldrich was used for catalyzing H_2O_2 to trigger the etching of GNRs. The magnetic nanoparticles with the diameter of 180 nm from Allrun

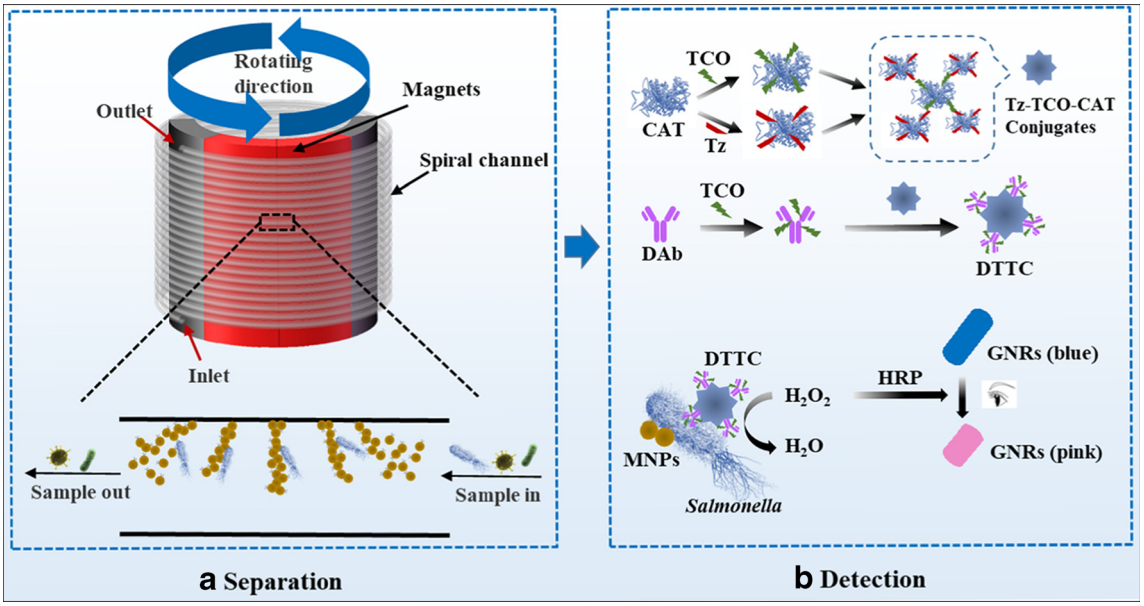

Fig. 1 Schematic of this colorimetric immunosensor for sensitive and rapid determination of *Salmonella* Typhimurium

Nano (Shanghai, China, http://www.allrunnano.com) were used for magnetic separation of the target bacteria. The polyclonal CAbs against *Salmonella* Typhimurium (*S.* typhimurium) from Abcam (Cambridge, MA, USA, https://www.abcam.com) were used to specifically capture the target bacteria. The monoclonal DAbs against *S.* typhimurium from Meridian (Memphis, TN, USA, https://meridianlifescience.com) were conjugated with the CATs and used for labeling the target bacteria. TCO-PEG4-NHS ester (TCO) and tetrazine-sulfo-NHS ester (Tz) from Click Chemistry Tools Bioconjugate Technology (Scottsdale, AZ, USA, https://clickchemistrytools.com) were used for click chemistry reaction between the Dabs and the CATs. Ultrapure water was obtained from Millipore Advantage 10 (18.2 MΩ·cm, Billerica, MA, USA, http://www.merckmillipore.com) and used for preparing all the solutions.

Development of the rotating immunomagnetic separator

The rotating immunomagnetic separator played a crucial role in this colorimetric immunosensor. It consisted of two main parts: (1) a rotating high gradient magnetic field for anti-clockwise moving of the magnetic nanoparticles and (2) a spiral FEP (fluorinated ethylene propylene) tubing channel for clockwise transfer of the bacteria samples. The high gradient magnetic field was generated by setting up two repelling arc magnets (material, NdFeB; grade, N40; inner diameter, 15 mm; outer diameter, 20 mm; height, 40 mm; arc angle, 90°; magnetization direction, through circumference) in an aluminum cylinder holder (radium, 20 mm; height, 45 mm). The arc magnets were tailor-made by Dachang Magnetics (Xuzhou, Jiangsu, China). The holder was anti-clockwise rotated using a stepping motor and a microcontroller. The spiral channel with the turn of 20 was formed by surrounding the cylinder holder with a FEP tubing (inner diameter, 0.5 mm; outer diameter, 1.6 mm). The inlet and outlet of the channel were connected with a peristaltic pump (T60-S2&WX10-14-A, flowrate, 0–24 mL min^{-1}, Longer Pump, Baoding, China) for pumping the solution and a centrifuge tube for collecting the waste, respectively.

Separation of the target bacteria

The separation of the target bacteria from a large-volume (10 mL) sample was the key to this immunosensor and conducted using the rotating magnetic separator. Before magnetic separation, the spiral channel was successively rinsed with 75% alcohol and deionized water, followed by blocking with 1% BSA for 30 min and washed with sterile PBS. For the magnetic separation of the target bacteria, 50 μg of the immune MNPs, which were prepared according to the protocol in the supplemental material, were first suspended in 300 μL of PBS and injected into the spiral channel, and the magnetic field was anti-clockwise rotated at a speed of 5 rpm. Then, 10 mL of the bacterial sample at each concentration from 10^1 to 10^6 CFU mL^{-1} was injected into the channel with a flow rate of 150 μL min^{-1}. The target bacteria were captured by the immune MNPs in the channel to form the magnetic bacteria through antigen-antibody binding. After 10 mL of the sample completely flowed through the channel, 1 mL of sterile PBST (PBS with 0.05% Tween-20) was injected into the channel for washing. Finally, the magnetic field was removed and another 1 mL of sterile PBS was used to collect the magnetic bacteria for detection.

Detection of the target bacteria

The detection of the target bacteria was based on enzymatic bacteria formation, CAT catalysis, and optical measurement. First, 100 μL of DAb-TCO-Tz-CAT conjugates (DTTCs, 0.4 mg mL^{-1}), which were synthesized according to the protocol in the supplemental material, was incubated with 1 mL of the magnetic bacteria for 45 min to form the enzymatic bacteria. Then, the mixture was washed three times with PBST to remove the unbound DTTCs, and 100 μL of H_2O_2 (0.2 mM) was added and catalyzed by the CAT on the enzymatic bacteria for 10 min. After magnetic separation for 2 min to collect the supernatant, 100 μL of the chromogenic solution (containing 5 μL of 4 mg mL^{-1} HRP, 5 μL of 0.5 mM CTAB, 5 μL of sodium acetate-acetic acid buffer, and 85 μL of GNRs, which were prepared according to the protocol in the supplemental material) was added into the supernatant and incubated for 20 min. This resulted in the change on the color of the solution from dark blue to pink. Finally, the absorbance peak shift was measured using a microplate reader (Infinite 200 PRO, TECAN, Grodig, Austria) to determine the concentration of the target bacteria.

Besides, the chicken samples purchased from the local supermarket were spiked with pure *S.* typhimurium at different concentrations and detected using this immunosensor. According to China's food safety national standards, 25 g of the chicken sample was first added into 225 mL of PBS and homogenized for 4 min using a stomacher (BagMixer CC, InterScience, Paris, France). Then, the supernatant was collected and placed at 4 °C for about 10 min. Different concentrations (10^2–10^5 CFU mL^{-1}) of the spiked chicken samples (10 mL) were prepared by adding the *S.* typhimurium cells into the supernatant. Finally, the spiked chicken samples were separated by this rotating magnetic separator and detected by this immunosensor.

Expression of the absorbance peak shift

This immunosensor was based on the etching of the GNRs, which can result in the absorbance peak shift. Thus, $\triangle\lambda$ was used to express the absorbance peak shift for data analysis in this study and can be described as:

$$\Delta\lambda = \lambda_1 - \lambda_0 \quad (1)$$

where λ_1 and λ_0 are the absorbance peaks after and before etching, respectively.

Results and discussions

Quantitative measurement of H_2O_2

This immunosensor was based on quantitative measurement of H_2O_2 using the etching of GNRs, which was triggered by •OH from the HRP + H_2O_2 system. To understand the quantitative detection range, different concentrations of H_2O_2 from 0 to 200 μM were used to etch the same amount of the GNRs (100 μL) when the concentration of HRP was 100 μg mL^{-1}. As shown in Fig. 2a, the color of the GNRs changes from dark blue to blue, then to purple, and finally to pink with the concentration of H_2O_2 increases from 0 to 200 μM, because more •OH were generated to etch the GNRs, resulting in larger changes in the shape of the GNRs. As can be also seen from Fig. 2b, the absorbance peak shifts toward blue and the absorbance decreases with the increase of H_2O_2 concentration. A good linear relationship between the peak shift ($\Delta\lambda$) and the concentration of H_2O_2 (C) is found (Fig. 2c) and can be expressed as $\Delta\lambda = 0.5551C + 3.9763$ ($R^2 = 0.9979$), indicating that the peak shift can be used for quantitative measurement of H_2O_2 at the range of 20–200 μM. Besides, transmission electron microscopy (TEM) was used to observe the change on the GNRs for different concentrations (0, 40, and 80 μM) of H_2O_2. As shown in Fig. 2d–f, the length of the GNRs decreases with the increase of H_2O_2 concentration because more •OH are generated from the reaction between HRP and H_2O_2 to etch the GNRs, and this also verifies the successful etching of the GNRs.

Simulation of the magnetic field

For this immunosensor, it is of great importance to rotate the immune MNPs in the opposite fluid direction for capturing the target bacteria. When the target bacteria were separated using this rotating magnetic separator with the immune MNPs, the MNPs in the spiral channel are subject to two main forces: the fluidic drag from the fluidic sample and the magnetic force from the magnetic field. The fluidic drag F_d can be expressed by Stoke's law as

$$F_d = 6\pi\eta r v \quad (2)$$

where η is the viscosity of the fluid, r is the radius of the particle, and v is the velocity of the fluid.

The magnetic force F_m can be expressed as

$$F_m = \mu_0 \chi V H \nabla H \quad (3)$$

where χ is the difference between the volume magnetic susceptibility of the particle and the surrounding fluid, $\mu_0 = 4\pi \times 10^{-7}$ Wb·$(Am)^{-1}$ is the magnetic permeability of vacuum, V is the volume of the particle, and H and ∇H are the strength and gradient of the magnetic field, respectively [29].

To rotate the immune MNPs, a high strength and gradient magnetic field is essential to provide a strong magnetic force since the magnetic force is proportional to the strength and gradient of the magnetic field. Thus, the Finite Element Method Magnetics (FEMM) software was used to simulate

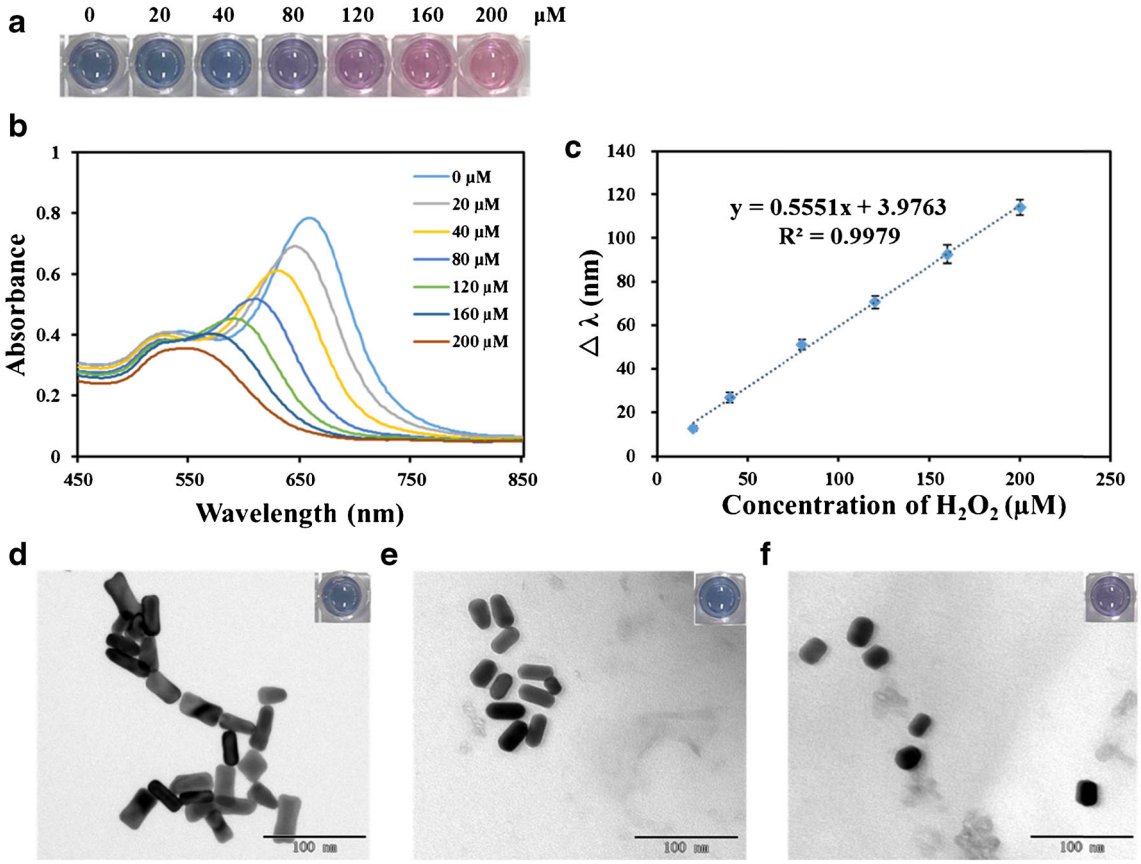

Fig. 2 **a** The visible color change of the GNRs for different concentrations of H_2O_2. **b** The absorbance spectra of the GNRs for different concentrations of H_2O_2. **c** The linear relationship between the absorbance peak shift and the concentration of H_2O_2 ($N = 3$). **d**–**f** The TEM images of the GNRs for different concentrations (0, 40, and 80 μM) of H_2O_2

the magnetic field generated by two arc magnets in mutual repelling layout. As shown in Fig. 3, a high gradient and strength magnetic field is generated in the spiral channel. The mean strength of the magnetic field in the spiral channel (from A to B) is about 0.77 T, and the gradient of the magnetic field is up to 337 T m^{-1}. This strong magnetic field is strong enough to rotate the immune MNPs in the opposite fluidic channel.

Optimization of magnetic separation of the target bacteria

For magnetic separation of the target bacteria, the following parameters were optimized: (a) the flow rate of the sample, (b) the rotating speed of the magnetic field, and (c) the amount of the immune MNPs. More detailed information on the optimization of these parameters could

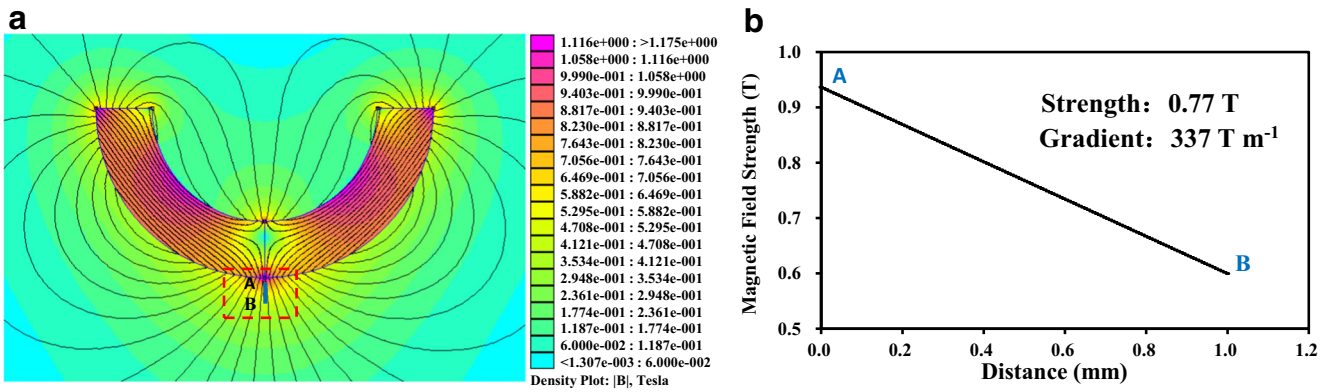

Fig. 3 **a** Simulation of the magnetic field. **b** The strength of the magnetic field in the spiral channel

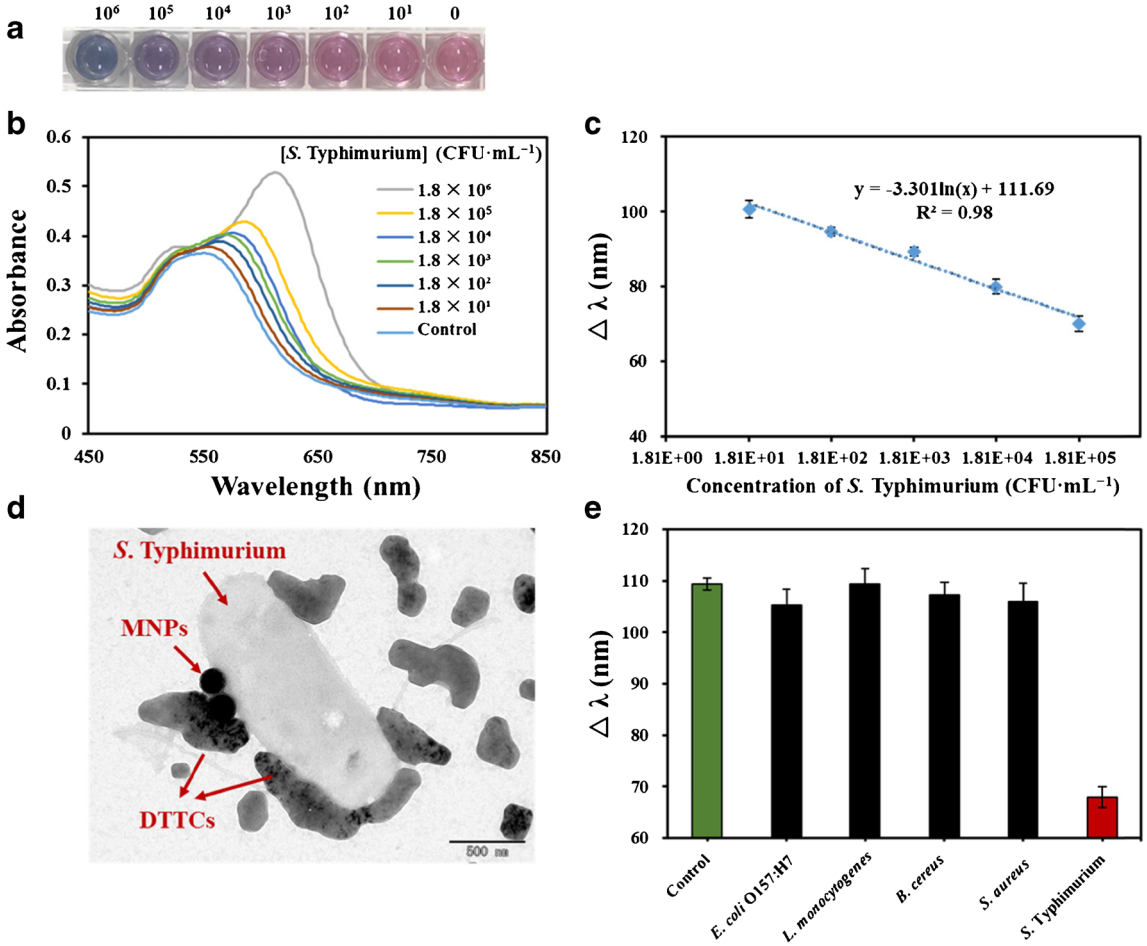

Fig. 4 **a** The color change of the GNRs for the determination of *S.* typhimurium with different concentrations. **b** The absorbance spectra of the GNRs for the determination of *S.* typhimurium with different concentrations. **c** Linear calibration model of this immunosensor for the determination of *S.* typhimurium ranging from 10^1 CFU mL^{-1} to 10^5 CFU mL^{-1}. **d** The TEM image of the MNP-bacteria-DTTC sandwich complex. **e** The specificity of this immunosensor for the determination of *S.* typhimurium, *E. coli* O157:H7, *L. monocytogenes*, *B. cereus*, and *S. aureus* at the same concentration of 10^5 CFU mL^{-1}, and the negative control ($N = 3$)

be found in the supplemental material. In short, the following experimental conditions were found to give the best results: (a) optimal sample flow rate, 150 μL min^{-1}; (b) optimal rotating speed, 5 rpm; and (c) optimal amount of immune MNPs, 50 μg.

Optimization of colorimetric detection of the target bacteria

For colorimetric detection of the target bacteria, the following parameters were optimized: (a) the etching time of the GNRs,

Table 1 Comparison of this immunosensor with reported optical methods for the determination of pathogenic bacteria

Sample volume	Signal indicator	Target bacteria	LOD (CFU mL^{-1})	References
0.01 mL	Quantum dots	*Vibrio anguillarum*	1.0×10^3	[30]
0.1 mL	TMB	*Staphylococcus aureus*	2.5×10^3	[31]
0.5 mL	AuNP@SWCNT*	*Escherichia coli*	1.0×10^2	[32]
1 mL	Gold nanoparticles	*Cronobacter sakazakii*	7.1×10^3	[33]
1 mL	Blue silica nanoparticles	*Salmonella*	8.8×10^1	[34]
1 mL	Gold nanorods	*Listeria monocytogenes*	1.0×10^1	[35]
10 mL	TMB	*Escherichia coli* O157:H7	1.0×10^2	[36]
10 mL	Gold nanorods	*Salmonella* Typhimurium	3.5×10^1	This study

*AuNP@SWCNT, gold nanostructure attached single-walled carbon nanotubes

(b) the concentration of H_2O_2, and (c) the concentration of the DTTCs. More detailed information on the optimization of these parameters could also be found in the supplemental material. In short, the following experimental conditions were found to give best results: (a) optimal etching time, 20 min; (b) optimal concentration of H_2O_2, 0.2 mM; and (c) optimal concentration of the DTTCs, 0.4 mg mL^{-1}.

Analytical performance of this immunosensor

Under the optimal conditions, different concentrations of *S.* typhimurium (1.8×10^1 CFU mL^{-1} to 1.8×10^6 CFU mL^{-1}) were detected using this immunosensor to evaluate its analytical performance. Figure 4a shows that the color of the GNRs changes from blue first to purple and then to pink, which can be distinguished visually, when the concentration of *S.* typhimurium increases from 1.8×10^1 CFU mL^{-1} to 1.8×10^6 CFU mL^{-1}. The absorbance spectra of the GNRs were further measured using the microplate reader and shown in Fig. 4b. From Fig. 4c, the absorbance peak shift is observed to be linear with the concentration of *S.* typhimurium from 1.8×10^1 CFU mL^{-1} to 1.8×10^5 CFU mL^{-1}. The low detection limit of this immunosensor was calculated to be 35 CFU mL^{-1} based on three times of signal-to-noise ratio. Besides, transmission electron microscopy was used to further confirm the formation of the MNP-bacteria-DTTC sandwich complexes (see Fig. 4d).

The specificity of this immunosensor was investigated by detecting four common pathogenic bacteria at the concentration of 10^5 CFU mL^{-1}, including *E. coli* O157:H7, *Listeria monocytogenes*, *B. cereus*, and *S. aureus*. Sterile PBS was used as a negative control. As shown in Fig. 4e, no remarkable change on the absorbance peak shift is observed for the non-target bacteria samples and the negative control sample, compared to the target bacteria at the same concentration of 10^5 CFU mL^{-1}. This indicated that this immunosensor had a good specificity toward *S.* typhimurium.

Compared with some reported optical methods for the detection of foodborne pathogenic bacteria (see Table 1), this immunosensor had a lower or comparable detection limit. The high sensitivity of this immunosensor may be attributed to the following aspects: (1) specific separation and efficient concentration of the target bacteria from a large volume of bacterial sample using the rotating magnetic separator, (2) effective amplification of the biological signals using click chemistry and CAT to catalyze H_2O_2, and (3) sensitive measurement of the remaining H_2O_2 using HRP and GNRs. The biggest difference between this immunosensor and these reported methods is this rotating magnetic separator, which has shown its great merits over the conventional magnetic separators, including (1) the moving immune MNPs can better react with the fluidic target bacteria in the opposite fluidic direction, (2) this separator can separate the target bacteria from a large volume of sample (up to 10 mL) while the conventional separators can only handle the sample with the volume less than 1 mL, and (3) this separator has a much stronger magnetic field with a mean magnetic intensity of ~ 0.77 T and a mean gradient of ~ 337 T m^{-1} while the conventional separators often have a magnetic intensity of 0.3–0.5 T and a mean gradient of < 100 T m^{-1}.

To further investigate the applicability of this immunosensor for the determination of *S.* typhimurium, chicken samples spiked with different concentrations of *S.* typhimurium (1.8×10^2 CFU mL^{-1} to 1.8×10^5 CFU mL^{-1}) were tested using this immunosensor. As shown in Table S1, the recoveries of the target bacteria at different concentrations (1.8×10^2 CFU mL^{-1} to 1.8×10^5 CFU mL^{-1}) are 103%, 101%, 114%, and 117%, respectively, with the mean recovery of 109%, indicating the feasibility of this immunosensor for the determination of *S.* typhimurium in chicken samples.

Conclusions

In this study, a colorimetric immunosensor was successfully developed for rapid determination of *Salmonella* Typhimurium using the rotating magnetic field with immunomagnetic nanoparticles to separate the target bacteria from large volume, the Tz/TCO click chemistry to amplify the biological signals, and the gold nanorods to indicate the detection results. This immunosensor had exhibited a satisfactory sensitivity and specificity for *Salmonella* Typhimurium. The new rotating magnetic separator was demonstrated to be effective for continuous-flow separation of target bacteria from large volume using a small amount of magnetic nanoparticles. However, the separation time is a little long and might be shortened using larger-sized magnetic nanoparticles with faster flow rate and stronger magnetic field. Besides, the optical detection was still dependent on benchtop instrument and might be improved using smartphone App to identify the color change. This immunosensor has the potential for visual detection of other foodborne bacteria using their specific biological recognition elements.

Funding information This study was supported in part by National Key Research and Development of China (2016YFD0500900), Walmart Foundation (SA1703161), and Walmart Food Safety Collaboration Center.

Compliance with ethical standards

Conflict of interest The authors declare that they have no conflict of interest.

References

1. Liu H, Dong H, Chen Z, Lin L, Chen H, Li S, Deng Y (2017) Magnetic nanoparticles enhanced microarray detection of multiple foodborne pathogens. J Biomed Nanotechnol 13(10):1333–1343. https://doi.org/10.1166/jbn.2017.2418
2. Silva NFD, Magalhaes J, Freire C, Delerue-Matos C (2018) Electrochemical biosensors for *Salmonella*: state of the art and challenges in food safety assessment. Biosens Bioelectron 99: 667–682. https://doi.org/10.1016/j.bios.2017.08.019
3. Vinayaka AC, Ngo TA, Kant K, Engelsmann P, Dave VP, Shahbazi MA, Wolff A, Bang DD (2019) Rapid detection of *Salmonella enterica* in food samples by a novel approach with combination of sample concentration and direct PCR. Biosens Bioelectron 129:224–230. https://doi.org/10.1016/j.bios.2018.09.078
4. Lungu B, Waltman WD, Berghaus RD, Hofacre CL (2012) Comparison of a real-time PCR method with a culture method for the detection of *Salmonella enterica* serotype Enteritidis in naturally contaminated environmental samples from integrated poultry houses. J Food Prot 75(4):743–747. https://doi.org/10.4315/0362-028X
5. Ma Z, Yang X, Fang Y, Tong Z, Lin H, Fan H (2017) Detection of *Salmonella* infection in chickens by an indirect enzyme-linked immunosorbent assay based on presence of PagC antibodies in sera. Foodborne Pathog Dis 15(2). https://doi.org/10.1089/fpd.2017.2322
6. Bunroddith K, Viseshakul N, Chansiri K, Lieberzeit P (2018) QCM-based rapid detection of PCR amplification products of *Ehrlichia canis*. Anal Chim Acta 1001:106–111. https://doi.org/10.1016/j.aca.2017.10.037
7. Zhang Z, Wang H, Chen Z, Wang X, Choo J, Chen L (2018) Plasmonic colorimetric sensors based on etching and growth of noble metal nanoparticles: strategies and applications. Biosens Bioelectron 114:52–65. https://doi.org/10.1016/j.bios.2018.05.015
8. Xu X, Ma X, Wang H, Wang Z (2018) Aptamer based SERS detection of *Salmonella* Typhimurium using DNA-assembled gold nanodimers. Microchim Acta 185(7):325. https://doi.org/10.1007/s00604-018-2852-0
9. Dai G, Li Z, Luo F, Ai S, Chen B, Wang Q (2019) Electrochemical determination of *Salmonella* Typhimurium by using aptamer-loaded gold nanoparticles and a composite prepared from a metal-organic framework (type UiO-67) and graphene. Microchim Acta 186(9):620. https://doi.org/10.1007/s00604-019-3724-y
10. Satija J, Punjabi N, Mishra D, Mukherji S (2016) Plasmonic-ELISA: expanding horizons. RSC Adv 6(88):85440–85456. https://doi.org/10.1039/c6ra16750k
11. Wang D, Guo R, Wei Y, Zhang Y, Zhao X, Xu Z (2018) Sensitive multicolor visual detection of telomerase activity based on catalytic hairpin assembly and etching of Au nanorods. Biosens Bioelectron 122:247–253. https://doi.org/10.1016/j.bios.2018.09.064
12. Yu X, Lin Y, Wang X, Xu L, Wang Z, Fu F (2018) Exonuclease-assisted multicolor aptasensor for visual detection of ochratoxin a based on G-quadruplex-hemin DNAzyme-mediated etching of gold nanorod. Microchim Acta 185(5):259. https://doi.org/10.1007/s00604-018-2811-9
13. Lin Y, Xu S, Yang J, Huang Y, Chen Z, Qiu B, Lin Z, Chen G, Guo L (2018) Interesting optical variations of the etching of Au Nanobipyramid@Ag Nanorods and its application as a colorful chromogenic substrate for immunoassays. Sensors Actuators B Chem 267:502–509. https://doi.org/10.1016/j.snb.2018.04.060
14. Gao L, Zhuang J, Nie L, Zhang J, Zhang Y, Gu N, Wang T, Feng J, Yang D, Perrett S, Yan X (2007) Intrinsic peroxidase-like activity of ferromagnetic nanoparticles. Nat Nanotechnol 2(9):577–583. https://doi.org/10.1038/nnano.2007.260
15. Saa L, Coronado-Puchau M, Pavlov V, Liz-Marzan LM (2014) Enzymatic etching of gold nanorods by horseradish peroxidase and application to blood glucose detection. Nanoscale 6(13): 7405–7409. https://doi.org/10.1039/c4nr01323a
16. Ren X, Ma H, Zhang T, Zhang Y, Yan T, Du B, Wei Q (2017) Sulfur-doped graphene-based immunological biosensing platform for multianalysis of cancer biomarkers. ACS Appl Mater Interfaces 9(43):37637–37644. https://doi.org/10.1021/acsami.7b13416
17. Chen Y, Xianyu Y, Wu J, Yin B, Jiang X (2016) Click chemistry-mediated nanosensors for biochemical assays. Theranostics 6(7): 969–985. https://doi.org/10.7150/thno.14856
18. Wu L, Xianyu Y, Wang Z, Dong Y, Hu X, Chen Y (2019) Amplified magnetic resonance sensing via enzyme-mediated click chemistry and magnetic separation. Anal Chem 91(24):15555–15562. https://doi.org/10.1021/acs.analchem.9b03550
19. Dong Y, Zheng W, Chen D, Li X, Wang J, Wang Z, Chen Y (2019) Click reaction-mediated T2 immunosensor for ultrasensitive detection of pesticide residues via brush-like nanostructure-triggered coordination chemistry. J Agric Food Chem 67(35):9942–9949. https://doi.org/10.1021/acs.jafc.9b03463
20. Ran B, Xianyu Y, Dong M, Chen Y, Qian Z, Jiang X (2017) Bioorthogonal reaction-mediated ELISA using peroxide test strip as signal readout for point-of-care testing. Anal Chem 89(11): 6113–6119. https://doi.org/10.1021/acs.analchem.7b00831
21. Xianyu Y, Dong Y, Wang Z, Xu Z, Huang R, Chen Y (2019) Broad-range magnetic relaxation switching bioassays using click chemistry-mediated assembly of polystyrene beads and magnetic nanoparticles. ACS Sens 4(7):1942–1949. https://doi.org/10.1021/acssensors.9b00900
22. Jiang X, Xianyu Y, Wu J, Chen Y, Zheng W, Xie M (2018) Controllable assembly of enzymes for multiplexed lab-on-a-chip bioassays with tunable detection range. Angew Chem Int Ed 130(25). https://doi.org/10.1002/anie.201801815
23. Yang Y, Xu F, Xu H, Aguilar ZP, Niu R, Yuan Y, Sun J, You X, Lai W, Xiong Y (2013) Magnetic nano-beads based separation combined with propidium monoazide treatment and multiplex PCR assay for simultaneous detection of viable *Salmonella* Typhimurium, *Escherichia coli* O157:H7 and *Listeria monocytogenes* in food products. Food Microbiol 34(2):418–424. https://doi.org/10.1016/j.fm.2013.01.004
24. Chen J, Shi X, Gehring AG, Paoli GC (2014) Automated immunomagnetic separation for the detection of *Escherichia coli* O157:H7 from spinach. Int J Food Microbiol 179(22):33–37. https://doi.org/10.1016/j.ijfoodmicro.2014.03.022
25. Lee W, Kwon D, Chung B, Jung GY, Au A, Folch A, Jeon S (2014) Ultrarapid detection of pathogenic bacteria using a 3D immunomagnetic flow assay. Anal Chem 86(13):6683–6688. https://doi.org/10.1021/ac501436d
26. Armbrecht L, Dincer C, Kling A, Horak J, Kieninger J, Urban G (2015) Self-assembled magnetic bead chains for sensitivity enhancement of microfluidic electrochemical biosensor platforms. Lab Chip 15(22):4314–4321. https://doi.org/10.1039/c5lc00796h
27. Cai G, Wang S, Zheng L, Lin J (2018) A fluidic device for Immunomagnetic separation of foodborne bacteria using self-assembled magnetic nanoparticle chains. Micromachines 9(12). https://doi.org/10.3390/mi9120624
28. Huang F, Zhang H, Wang L, Lai W, Lin J (2018) A sensitive biosensor using double-layer capillary based immunomagnetic separation and invertase-nanocluster based signal amplification for rapid detection of foodborne pathogen. Biosens Bioelectron 100:583–590. https://doi.org/10.1016/j.bios.2017.10.005
29. Lin J, Li M, Li Y, Chen Q (2015) A high gradient and strength bioseparator with nano-sized immunomagnetic particles for specific separation and efficient concentration of *E. coli* O157:H7. J Magn Magn Mater 378:206–213. https://doi.org/10.1016/j.jmmm.2014.11.039

30. Zhang Y, Xiao J, Wang Q, Zhang Y (2016) A modified quantum dot-based dot blot assay for rapid detection of fish pathogen *Vibrio anguillarum*. J Microbiol Biotechnol 26(8):1457–1463. https://doi.org/10.4014/jmb.1602.02050
31. Yan C, Zhang Y, Yang H, Yu J, Wei H (2017) Combining phagomagnetic separation with immunoassay for specific, fast and sensitive detection of *Staphylococcus aureus*. Talanta 170: 291–297. https://doi.org/10.1016/j.talanta.2017.04.007
32. Ondera TJ, Hamme Ii AT (2015) Magnetic-optical nanohybrids for targeted detection, separation, and photothermal ablation of drug-resistant pathogens. Analyst 140(23):7902–7911. https://doi.org/10.1039/c5an00497g
33. Kim H-S, Kim Y-J, Chon J-W, Kim D-H, Yim J-H, Kim H, Seo K-H (2017) Two-stage label-free aptasensing platform for rapid detection of *Cronobacter sakazakii* in powdered infant formula. Sensors Actuators B Chem 239:94–99. https://doi.org/10.1016/j.snb.2016.07.173
34. Sun Q, Zhao G, Dou W (2016) An optical and rapid sandwich immunoassay method for detection of *Salmonella* pullorum and *Salmonella* gallinarum based on immune blue silica nanoparticles and magnetic nanoparticles. Sensors Actuators B Chem 226:69–75. https://doi.org/10.1016/j.snb.2015.11.117
35. Liu Y, Wang J, Zhao C, Guo X, Song X, Zhao W, Liu S, Xu K, Li J (2019) A multicolorimetric assay for rapid detection of *Listeria monocytogenes* based on the etching of gold nanorods. Anal Chim Acta 1048:154–160. https://doi.org/10.1016/j.aca.2018.10.020
36. Ren W, Liu W, Irudayaraj J (2017) A net fishing enrichment strategy for colorimetric detection of *E. coli* O157:H7. Sensors Actuators B Chem 247:923–929. https://doi.org/10.1016/j.snb.2017.03.090